Advances in Applied Mathematics and Mechanics
Adv. Appl. Math. Mech., Vol. **2**, No. 5, pp. 677-684

DOI: 10.4208/aamm.10-10S10
October 2010

Lattice Boltzmann Method for Thermocapillary Flows

Lin Zheng[1], Zhaoli Guo[1,*], Baochang Shi[1] and Chuguang Zheng[1]

[1] *National Laboratory of Coal Combustion, Huazhong University of Science and Technology, Wuhan 430074, China*

Received 5 March 2010; Accepted (in revised version) 3 April 2010
Available online 13 July 2010

Abstract. In this paper, we apply a recently proposed thermal axisymmetric lattice Boltzmann model to the thermocapillary driven flow in a cylindrical container. The temperature profiles and isothermal lines at the free surface with Prandtl (Pr) number fixed at 0.01 and Marangoni (Ma) number varying from 10 to 500 are measured and compared with the previous numerical results. In addition, we also give the numerical results for different Ma numbers at Pr=1.0. It is shown that present results greed well with those reported in previous studies.

AMS subject classifications: 65C20, 80A20, 76R10
Key words: Lattice Boltzmann method, axisymmetric flows, thermocapillary flows.

---

1 Introduction

Surface tension gradient at a free surface could induce a viscous driving flow [1–3]. This phenomena (usually called thermocapillary convection) is often encountered in many industrial processes. The subject of thermocapillary convection has been an interesting area for the science and engineering due to its complex flow filed and practical applications such as crystal growth melts and the convective flows in the microgravity environment.

In some special cases, e.g., thermocapillary convection in an axisymmetric configuration, such flows can be regarded as a quasi-two-dimensional problems. Many traditional methods such as finite difference method, finite volume method, vorticity-stream method, SIMPLE method have been applied to this field. It should be mentioned that, in the last two decades, lattice Boltzmann equation (LBE) has been rapidly developed as an effective and promising numerical algorithm for computational fluid dynamics [4–6], which has also been applied to axisymmetric flows [7–12].

Thermocapillary flow induced by the temperature gradient in the rectangular cavity has been widely studied by traditional methods and LBE. However, to the authors'

---

*Corresponding author.
Email: zlguo@mail.hust.edu.cn (Z. L. Guo)

acknowledge, there are many attempts to apply the traditional methods to the thermocapillary flow in an axisymmetric cylindrical cavity, but it's quite rare for LBE. Therefore, in present paper, we will apply a recent thermal axisymmetric model [11] to the thermocapillary driven flow in a cylindrical container by a motionless surface with constant wall temperature and straight, undeformable lateral free surface boundary with a steady heat flux. Numerical simulations have been conducted at different Pr and Ma numbers and the numerical results indicate that present results agree well with other existing work [1].

The outline of the paper is as follows: in Section 2 we give a brief description of the physical problem. In Section 3 the axisymmetric thermal LBE model is introduced. Then we demonstrate some numerical simulations to validate the results in Section 4 and the conclusions are drawn in Section 5.

2 Physical problem description

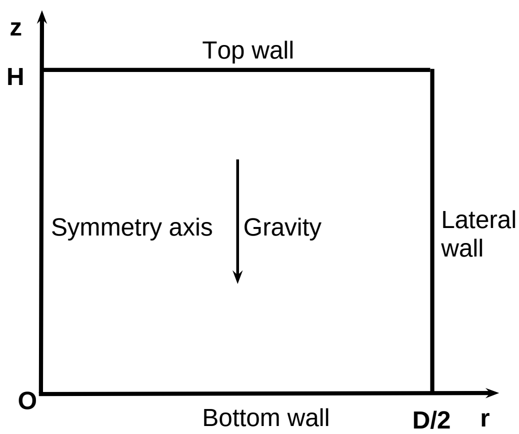

Figure 1: Sketch of the cylinder flow.

The physical configuration in Fig. 1 is axisymmetric, limited by motionless surface with constant wall temperature. The lateral boundary is the free surface which is taken to be straight and undeformable. The ratio of the radius and the height is fixed at 1/2, the gravity force and the azimuthal velocity is ignored in this case. Under these conditions, the liquid motion and temperature distribution for this problem are governed by the following dimensionless equations

$$\frac{1}{r}\frac{\partial(ru_r)}{\partial r}+\frac{\partial u_z}{\partial z}=0, \tag{2.1a}$$

$$\frac{\partial u_r}{\partial t}+u_r\frac{\partial u_r}{\partial r}+u_z\frac{\partial u_r}{\partial z}=-\frac{\partial p}{\partial r}+\mathrm{Pr}(\nabla^2 u_r-\frac{u_r}{r^2}), \tag{2.1b}$$

$$\frac{\partial u_z}{\partial t} + u_r\frac{\partial u_z}{\partial r} + u_z\frac{\partial u_z}{\partial z} = -\frac{\partial p}{\partial z} + \mathrm{Pr}\nabla^2 u_z, \tag{2.1c}$$

$$\frac{\partial T}{\partial t} + u_r\frac{\partial T}{\partial r} + u_z\frac{\partial T}{\partial z} = \nabla^2 T, \tag{2.1d}$$

where u_r and u_z are radial and axial velocity components, p is the pressure and T is temperature, Pr=ν/α is the Prandtl number with ν being viscosity coefficient and α the thermal diffusion coefficient, and

$$\nabla^2 = \frac{1}{r}\frac{\partial}{\partial r}\frac{r\partial}{\partial r} + \frac{\partial^2}{\partial z^2}.$$

The boundary conditions for this problem are the same as [1], which given as

$$\begin{cases} z=\pm 1: & u_r = u_z = 0, \;\; T = 0, \\ r = 1: & u_r = 0, \;\; \frac{\partial u_z}{\partial r} = -Ma\frac{\partial T}{\partial z}f(z), \quad \frac{\partial T}{\partial r} = q(z), \\ r=0: & u_r = 0, \;\; \frac{\partial u_z}{\partial r} = 0, \;\; \frac{\partial T}{\partial r} = 0, \end{cases}$$

where Ma is the Marangoni number, $f(z)$ is the regularizing function and $q(z)$ is heat flux. In the following study, these two function are given as

$$f(z) = (1-z^2)^2, \quad \text{and} \quad q(z) = f(z).$$

3 Thermal axisymmetric lattice Boltzmann model

In this paper, the two dimensional nine discrete velocities (D2Q9) and D2Q4 LBE model are employed to simulating the velocity and temperature fields respectively. The evolution equations for the axial, radial velocity, and the temperature field can be respectively written as [9,11]

$$f_i(\boldsymbol{x}+\boldsymbol{c}_i\delta t, t+\delta t) - f_i(\boldsymbol{x},t) = -\frac{1}{\tau_f}\Big(f_i(\boldsymbol{x},t) - f_i^{(eq)}(\boldsymbol{x},t)\Big) + \delta t\Big(1-\frac{1}{2\tau_f}\Big)F_i(\boldsymbol{x},t), \tag{3.1a}$$

$$g_k(\boldsymbol{x}+\boldsymbol{c}_k\delta t, t+\delta t) - g_k(\boldsymbol{x},t) = -\frac{1}{\tau_g}\Big(g_k(\boldsymbol{x},t) - g_k^{(eq)}(\boldsymbol{x},t)\Big) + \delta t G_k(\boldsymbol{x},t), \tag{3.1b}$$

where f_i and g_k are the density and temperature distribution functions, respectively. τ_f and τ_g are respectively the relaxation times for the hydrodynamic and thermodynamic fields. δt is the streaming time, the equilibrium functions $f_i^{(eq)}$ and $g_k^{(eq)}$ are given as [9,11]

$$f_i^{(eq)} = r\omega_i\rho\Big\{1+\frac{\boldsymbol{c}_i\cdot\boldsymbol{u}}{RT} + \frac{1}{2}\Big[\Big(\frac{\boldsymbol{c}_i\cdot\boldsymbol{u}}{RT}\Big)^2 - \frac{(\boldsymbol{u}\cdot\boldsymbol{u})}{RT}\Big]\Big\}, \tag{3.2a}$$

$$h_k^{(eq)} = rT\bar{\omega}_k\Big(1+\frac{\boldsymbol{c}_k\cdot\boldsymbol{u}}{c_{sT}^2}\Big), \tag{3.2b}$$

and the source terms are respectively given as

$$F_i = \frac{(\boldsymbol{c}_i - \boldsymbol{u}) \cdot \boldsymbol{a}}{RT} f_i^{(eq)}, \qquad G_k = \bar{\omega}_k [\boldsymbol{c}_k \cdot \boldsymbol{b}], \tag{3.3}$$

where ω_0=4/9, ω_{1-4}=1/9 and ω_{5-8}=1/36 are the weight coefficients,

$$\boldsymbol{a} = \Big(a_r = \frac{(1 - 2\tau_f u_r/r)RT}{r}, \quad a_z = 0 \Big)$$

is the acceleration, $\bar{\omega}_k$=1/4 is the corresponding weight coefficient,

$$\boldsymbol{b} = \big(b_r = (1 - 1/2\tau_g)T, \quad b_z = 0 \big),$$

and $c_{sT}=\sqrt{3RT/2}$ is the model parameter.

The macroscopic density ρ, the axial velocity u_z, radial velocity u_r, and temperature T can be computed by the conservation laws of mass, momentum and energy, which can be defined by the moments of the distribution functions as

$$\rho = \frac{1}{r} \sum_i f_i, \tag{3.4a}$$

$$\rho u_\alpha = \frac{r}{r^2 + (\tau_f - 0.5)\delta t^2 RT \delta_{\alpha r}} \Big\{ \sum_i c_{i\alpha} f_i + \frac{\delta t}{2} \rho RT \delta_{\alpha r} \Big\}, \tag{3.4b}$$

$$T = \frac{1}{r} \sum_k h_k. \tag{3.4c}$$

In this model, the energy equation is solved by a simple LBE without any velocity and temperature gradients in the source term, which could be easily realized. Through the Chapman-Enskog expansion, the correct axisymmetric hydrodynamic equations can be recovered by Eqs. (3.1a)-(3.3). The detailed derivation of these macroscopic equations can be found in [9, 11].

4 Numerical simulations

In this section, we applied the above mentioned axisymmetric thermal model to thermocapillary driven flow. In our simulation, we employed a 100 × 200 square meshes, and the symmetry boundary condition and non-equilibrium-extrapolation boundary treatment [13] are applied to symmetry axis and other boundaries respectively.

We first consider the case with Ma varying from 10 to 500 at Pr=0.01. To validate the model, the isothermal lines for Ma=10 is included in Fig. 2 together with the results of [1]. It is observed that two phenomena are in good agreement for this case. For the quantitative comparison, we compared the temperature distribution at the free surface in Fig. 3 with Ma=10, 100 and 500. It is found that the numerical results agreed well with the work of [1].

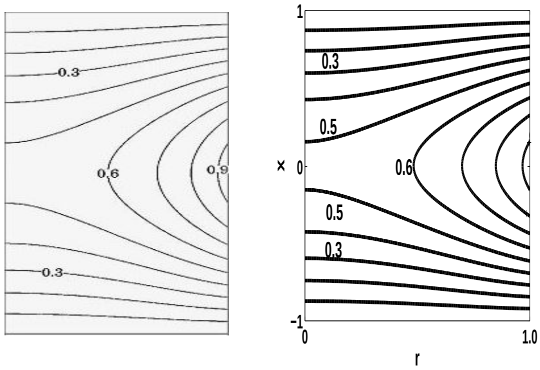

Figure 2: Isothermal lines at Pr=0.01, Ma=10. Left is from [1], right is the LBE results.

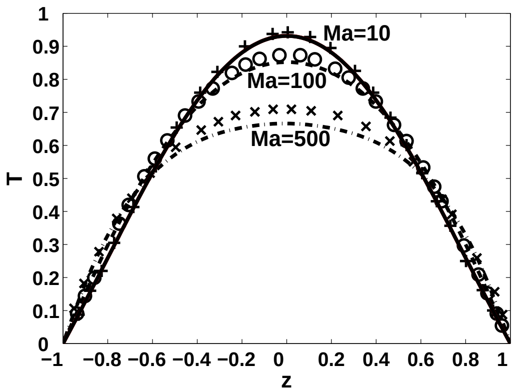

Figure 3: Temperature profiles at Pr=0.01 with Ma=10, 100, 500. Symbols are from [1], lines are the LBE results.

In Figs. 4 and 5, the streamlines and isothermal lines for Ma=10, 100 and 500 are also included. It is shown that the temperature field is much more affected by the velocity field as the Ma number increases. From Figs. 4 and 5, we observed that the vortexes are confined to the free surface, and the temperature field starts from conduction to convection as Ma number becomes large. These phenomena are also captured in [1].

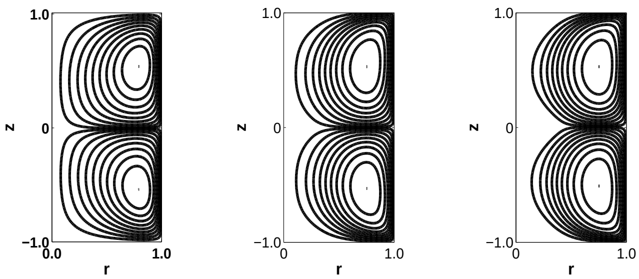

Figure 4: Streamlines at Pr=0.01. Left to right: Ma=10 ,100 and 500.

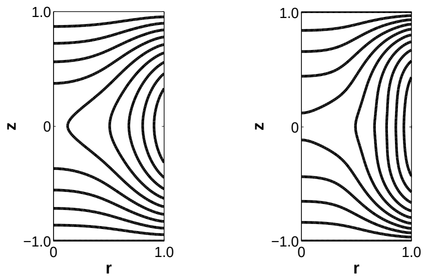

Figure 5: Isothermal lines at Pr=0.01. Left to right: Ma=100 and 500.

Next, we increase the Prandtl number to 1 with Ma number varying from 500 to 10000. The streamlines and isothermal lines for Ma=500, 5000 and 10000 are shown in Figs. 6 and 7. From the figures, It is shown that the contours of streamlines and isotherms are symmetric with respect to the mid-height plane at z=0 as the same phenomena as Pr=0.01 with Ma=10-500. In Figs. 5 and 7, the temperature field becomes more deformable as Prandtl number increases. Similar phenomena appear as Pr=0.01, the temperature field becomes more convective as the Ma number increases. In Fig. 8, the velocity distribution at free surface are plotted at the Pr=0.01 and 1 with different Ma numbers. As can be seen from Figs. 5 and 7, when the Ma number becomes large, the temperature become more deformable which also effects the velocity field, and the value of velocity is varying largely at the free surface as the Ma increased. These phenomena are also observed in [1].

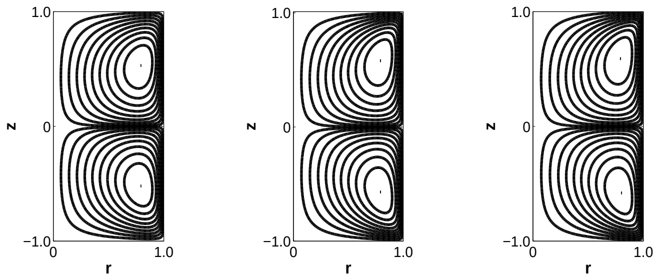

Figure 6: Streamlines at Pr=1. Left to right: Ma=500, 5000 and 10000.

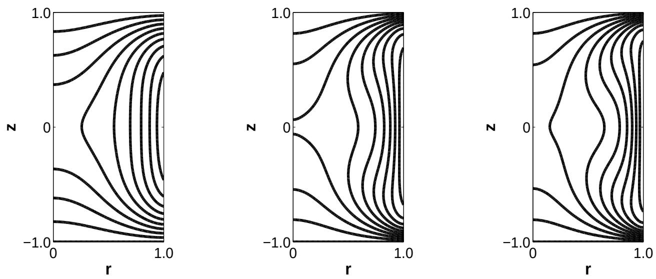

Figure 7: Isothermal lines at Pr=1. Left to right: Ma=500, 5000 and 10000.

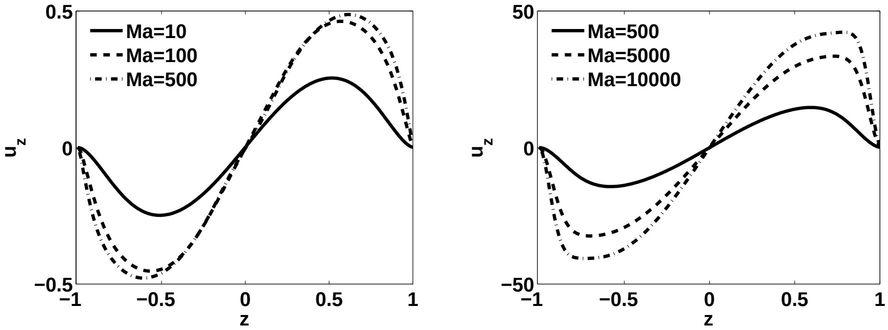

Figure 8: Velocity distribution at the free surface. Left to right: Pr=0.01 and 1.

5 Conclusions

In this paper, we have applied a thermal axisymmetric LBE model for axisymmetric thermocapillary driven flow with a lateral heated cylinder for different Prandtl and Marangoni numbers. In these cases, the temperature field is simulated by a simple D2Q4 LBE model without any velocity and temperature gradients in the source term. The temperature profiles and isothermal lines at the free surface with Prandtl (Pr) number fixed at 0.01 and Marangoni (Ma) number varying from 10 to 500 are measured, and the numerical results agree well with previous numerical results.

The contours of streamlines and isotherms are symmetric with respect to the mid-height plane at z=0. In addition, we also give the numerical results for different Ma numbers at Pr=1.0. It is shown that for low values of Ma, the isotherms are slightly deformed, and become much more deformed as Ma increased. These similar phenomena have also been observed in previous studies.

Acknowledgments

This work is supported by the National Natural Science Foundation of China (10972087 and 50721005) and the Basic Research Program of China (2006CB705800).

References

[1] G. Kasperski, A. Batoul and G. Labrosse, *Up to the unsteadiness of axisymmetric thermocapillary flows in a laterally heated liquid bridge*, Phys. Fluids., 12 (1) (2000), pp. 103–119.

[2] N. Kobayashi, *Computer simulation of the steady flow in a cylindrical float zone under low gravity*, J. Cryst. Growth., 66 (1984), pp. 63–72.

[3] H. C. Kuhlmann and H. J. Rath, *Hydrodynamic instabilities in cylindrical thermocapillary liquid bridges*, J. Fluid. Mech., 247 (1993), pp. 247–274 .

[4] R. Benzi, S. Succi and M. Vergassola, *The lattice Boltzmann equation: theory and applications*, Phys. Rep., 222 (1992), pp. 145–197.

[5] S. SUCCI, The Lattice Boltzmann Equation for Fluid Dynamics and Beyond, Oxford Univiversity Press, Oxford, 2001.

[6] S. CHEN AND G. DOOLEN, *Lattice Boltzmann method for fluid flows*, Annu. Rev. Fluid. Mech., 30 (1998), pp. 329–364.

[7] I. HALLIDAY, L. A. HAMMOND, C. M. CARE ET AL., *Lattice Boltzmann equation hydrodynamics*, Phys. Rev. E., 64 (2001), 011208.

[8] T. REIS AND T. N. PHILLIPS, *Numerical validation of a consistent axisymmetric lattice Boltzmann model*, Phys. Rev. E., 77 (2008), 026703.

[9] Z. L. GUO, H. F. HAN, B. C. SHI AND C. G. ZHENG, *Theory of the lattice Boltzmann equation: lattice Boltzmann model for axisymmetric flows*, Phys. Rev. E., 79 (2009), 046708.

[10] Y. PENG, C. SHU, Y. T. CHEW AND J. QIU, *Numerical investigation of flows in Czochralski crystal growth by an axisymmetric lattice Boltzmann method*, J. Comput. Phys., 186 (2003), pp. 295–307.

[11] L. ZHENG, Z. L. GUO, B. C. SHI AND C. G. ZHENG, *Lattice Boltzmann equation for axisymmetric thermal flows*, Comput. Fluids., 39 (2010), pp. 945–952.

[12] L. ZHENG, Z. L. GUO, B. C. SHI AND C. G. ZHENG, *Kinetic theory based lattice Boltzmann equation with viscous dissipation and pressure work for axisymmetric thermal flows*, J. Comput. Phys., 229 (2010), pp. 5843–5856.

[13] Z. L. GUO, C. G. ZHENG AND B. C. SHI, *An extrapolation method for boundary conditions in lattice Boltzmann method*, Phys. Fluids., 14 (2002), pp. 2007–2010.